

Molecular Analysis and Experimental Virulence of French and North American *Escherichia coli* Neonatal Meningitis Isolates: Identification of a New Virulent Clone

Stéphane Bonacorsi,¹ Olivier Clermont,¹ Véronique Houdouin,¹ Christophe Cordevant,³ Naima Brahim,¹ Armelle Marecat,³ Colin Tinsley,² Xavier Nassif,² Marc Lange,³ and Edouard Bingen¹

¹Laboratoire d'Études de Génétique Bactérienne dans les Infections de l'Enfant (EA 3105), Université Denis Diderot-Paris 7, Service de Microbiologie, Hôpital Robert Debré, and ²INSERM U570, Faculté de Médecine Necker-Enfants Malades, Paris, and ³Research and Development Division, Institut Pasteur de Lille, Lille, France

Phylogenetic relationships, virulence factors, alone and in specific combinations, and virulence in a rat meningitis model were examined among 132 isolates of *Escherichia coli* neonatal meningitis from France and North America. Isolates belonging to phylogenetic groups A ($n = 11$), D ($n = 20$), and B2 ($n = 99$) had similar high prevalence rates of the siderophores aerobactin and yersiniabactin and the K1 capsule ($\geq 70\%$) yet induced different level of experimental bacteremia. Ectochromosomal DNA-like domains involved in blood-brain barrier passage (PAI III₅₃₆ [*sfafoc* and *iroN*; 34%]; GimA [*ibeA* and *ptnC*; 38%]; PAI II₇₉₆ [*hly*, *cnf1*, and *hra*; 10%]) were restricted to B2 isolates. Among group B2 isolates, representatives of the O45:K1 clonal group ($n = 30$), which lacked these domains, were as able as the archetypal O18:K1 strain C5 to cause meningitis. Molecular epidemiology combined with experimental virulence assays demonstrate that known virulence factors are insufficient to fully explain the pathophysiology of ECNM and to allow for rational search for new virulence factors.

Bacterial meningitis is a major cause of neonatal mortality worldwide and is associated with a high incidence of neurologic sequelae [1]. *Escherichia coli* is the second cause of neonatal bacterial meningitis in industrialized countries, after group B streptococci (GBS), but may soon become the leading cause, with worldwide application of “per partum” antibacterial prophylaxis against GBS [2]. Moreover, several reports suggest that this preventive strategy is responsible for the increased in-

cidence of early-onset infection with *E. coli* [3–5]. This underlines the need for a better understanding of the molecular pathophysiology of *E. coli* neonatal meningitis (ECNM) to develop new preventive strategies.

The pathogenesis of ECNM is characterized by high-level bacteremia followed by penetration of the blood-brain barrier (BBB) [6–9]. The capsular polysaccharide K1 is a virulence factor with a key role in the bacteremic phase [10, 11]. Other bacterial attributes contribute to *E. coli* survival in serum and may thus be involved in the pathogenicity of ECNM isolates. These factors include iron-uptake systems encoded by the loci *iro* [12, 13] and *chu* [14], the siderophores aerobactin [15] and yersiniabactin [16–18], and other factors, such as hemolysin that may facilitate access to iron and or resistance to phagocytic cells [19–21]. Several specific virulence factors facilitate BBB penetration [9], such as

Received 18 September 2002; accepted 14 January 2003; electronically published 29 May 2003.

Reprints or correspondence: Prof. Edouard Bingen, Service de Microbiologie, Hôpital Robert Debré, 48 Blvd. Sérurier, 75395 Paris Cedex 19, France (edouard.bingen@rdb.ap-hop-paris.fr).

The Journal of Infectious Diseases 2003;187:1895–906

© 2003 by the Infectious Diseases Society of America. All rights reserved. 0022-1899/2003/18712-0009\$15.00

K1 [22], fimbrial adhesin S (*sfaS*) [23–25], the invasin IbeA (*ibeA*) [26, 27], and cytotoxic necrotizing factor (*cnf1*) [28, 29].

Extraintestinal pathogenicity genes in *E. coli* tend to be clustered in chromosomal genomic structures acquired by horizontal transfer and are known as “pathogenicity islands” (PAIs) [30] or genetic islands [31]. Recently, these structures were collectively termed “ectochromosomal DNA” (ECDNA) [32]. Some specific ECNM virulence factors were recently described as being linked to ECDNA, such as *sfaS* in PAI III₅₃₆ [33], *cnf1* in PAI II₉₆ [34] or PAI I_{C5} [35], and *ibeA* in the genetic island GimA [31]. The siderophores aerobactin and yersiniabactin, which are potentially involved in the bacteremic phase, are encoded by genes that may be included in such structures (PAI I_{CF1073} and high pathogenicity island [HPI], respectively) [18, 36–39]. These ECDNAs vary in length from 30 kb to >100 kb and include other potential virulence factors that may be involved in the pathogenesis of ECNM. Thus, epidemiological studies of ECDNA within meningitis isolates will contribute to the determination of genetic elements that are involved in the pathogenesis of ECNM.

The characterization and comparison of virulence genotypes (the complement of virulence genes and ECDNA present in a given strain), in association with phylogenetic analysis, will lead to a comprehensive picture of the origins and spread of virulence factors within the population of ECNM isolates. The application of this approach to a large collection of strains will permit the definitions of different archetypal groups that may be used to investigate the pathogenesis of this disease. Neonatal meningitis isolates mainly belong to phylogenetic group B2 [40, 41], a group of highly pathogenic isolates frequently involved in extraintestinal infection [36, 42–46], and, to a lesser extent, groups D and A. Although ECNM isolates belong to several clonal groups [40, 41, 47], most molecular and experimental analyses have involved small numbers of strains, all belonging to the main serotype (O18:K1) [47–49], which is considered to be the archetypal group. Determination of virulence genotypes and assessment of experimental virulence by use of bacterial isolates representative of other clonal groups, as well as comparison with the archetypal group O18:K1, may throw new light on the pathophysiology of ECNM.

Therefore, in the present study, we performed a phylogenetic analysis of a collection of 132 ECNM isolates of French and North American origins and screened them for the ECDNAs: PAI III₅₃₆ [33], PAI II₉₆ [34], GimA [31], PAI I_{CF1073} [36, 38], and HPI [16, 18, 39]. We also further characterized a recently identified meningitis-associated genomic region termed “GimB” [50] and determined its distribution in the isolate collection. Finally, the virulence of representative isolates belonging to different clusters or clonal groups was assessed in an animal model and was analyzed in comparison with the virulence genotypes harbored by the isolates.

MATERIALS AND METHODS

Isolates. We studied 134 isolates cultured from the cerebrospinal fluid (CSF) of 134 neonates from 1988–2000. Sixty-three of these isolates have been partially characterized in a study described elsewhere [40]. Ninety-one isolates were obtained from various regions of France. Forty-one North American isolates were provided by R. Bortolussi (Childrens’ Hospital, Halifax, Canada), D. Goldmann (Childrens’ Hospital, Boston), K. Kim (Johns Hopkins University School of Medicine, Baltimore), and J. Badger (Childrens Hospital Los Angeles) and included the archetypal O18:K1:H7 isolates RS218 and C5, which belong to the outer membrane protein pattern (OMP) 9 subclone [47]. For comparison, we also included the well-characterized European O18:K1:H7 isolates IHE3034 (OMP 9 subclone) and IHE3036 (OMP 6 subclone) [25, 47, 51] isolated in Finland and provided by J. Hacker (Institut für Molekulare Infektionsbiologie, Würzburg, Germany). All isolates were stored in 20% glycerol at –80°C.

Serotyping. K1 antigen was detected with antiserum to *Neisseria meningitidis* group B, as described elsewhere [40], and O antigens were screened for with antisera obtained from the State Serum Institute (Copenhagen, Denmark).

Polymerase chain reaction (PCR) phylogenetic grouping. The phylogenetic group was determined with a PCR-based method that detects the *chuA* and *yjaA* genes and an anonymous DNA fragment, TspE4.C2, as described elsewhere [52]. The distribution of these markers among *E. coli* phylogenetic groups categorized the isolates as follows: group A, *chuA*[–] and TspE4.C2[–]; group B1, *chuA*[–] and TspE4.C2⁺; group B2, *chuA*⁺ and *yjaA*⁺; and group D, *chuA*⁺ and *yjaA*[–].

Ribotyping. The isolates were automatically ribotyped by use of the Riboprinter system (Qualicon) with the restriction enzyme *Hind*III (New England BioLabs), as described elsewhere [53]. For comparison, ribotypes also were obtained by a manual method described elsewhere [40]. Computerized ribotypes were exported in .txt files, converted to .int files with GelConvert 1.01 software (Qualicon), and imported into Gel Compar software version 4.1 (Applied Maths). Clustering analysis was performed with the unweighted pair group method, using the arithmetic averages (unweighted pair group method with arithmetic mean [UPGMA]) method based on the Dice coefficient for band matching [54], with a position tolerance setting of 0.8% and an optimization setting of 0.25% (default values are 1% position tolerance and 0.5% optimization). Bands for analysis with the Dice coefficient were assigned manually, on the basis of densitometric curves and the accompanying hardcopy photograph. The ribotypes of the ECOR reference isolates [55], obtained with the same technique in a study described elsewhere [53], were compared with the ribotypes of the meningitis-associated *E. coli* (MENEC) isolates. All the ribotype profiles have been added to the electronic Riboprint

database that we have created, as described elsewhere [53]. With worldwide Riboprinter interconnection, this database provides an invaluable tool for rapidly determining genetic relationships between clinical ECNM isolates and isolates of this collection. The ribotypes can be downloaded from the Riboprinter database on electronic mail request to edouard.bingen@rdb.ap-hop-paris.fr or marc.lange@pasteur-lille.fr. All data obtained in this study (including dendrograms) are available at the Molecular Typing Center website (research section: <http://www.pasteur-lille.fr/english/techno/ctm/index.html>).

Pulsed-field gel electrophoresis (PFGE). PFGE was performed as described elsewhere [36]. In brief, bacterial cells were embedded in agarose and were lysed with detergent and proteinase K (Sigma-Aldrich). DNA was digested with *NotI* (Roche) and was subjected to PFGE in 1% agarose gel in 0.5× TBE buffer, at 6 V/cm for 27 h, with pulse times varying linearly between 2 s and 49 s.

ECDNA-like domains. ECDNA-like domains of PAI III₅₃₆ [33], GimA [31], PAI II_{J96} [34], PAI I_{CFT073} [36, 38], and HPI [16, 18] were detected by simultaneous identification of different characteristic genetic elements (table 1), using PCR, dot blot, and Southern blot, as follows. The isolates were first screened for the following genes by PCR: *sfa/foc*, *sfaS*, *iroN*, *ibeA*, *papC*, *papGII*, *papGIII*, *hlyC*, *cnf1*, *hra*, *iucC*, *fyuA*, and *irp2*. All the primers used in this study have been published elsewhere [36, 40, 43], except for those used for *iroN* (*iroN*.1, 5'-GAAAGCTCTGGTGGACGGTA-3'; and *iroN*.2, 5'-CGACAGAGGATTACCGGTGT-3'). The *ptnC* gene in GimA (table 1) was assessed by dot blot hybridization with the homologous subtractive clone SauE15.H10, as described elsewhere [50]. Because some of these genes have been described as belonging to different PAIs (e.g., *pap*, *hly*, and *iuc*) [30, 36], PFGE was used to determine the physical location and to show the physical linkage of genes representative of PAI III₅₃₆, PAI II_{J96}, and PAI I_{CFT073} (table 1). PFGE digests were transferred to nylon membranes (Amersham Pharmacia Biotech) and were hybridized

with digoxigenin-labeled probes. The probes were generated as recommended by the manufacturer (Roche), using primers specific for the following genes: *sfa/foc*, *iroN*, *papGII/III*, *hlyC*, *cnf1*, *hra*, and *iucC*. Finally, the insertion sites of the PAI II_{J96}-like domain and the HPI-like domain were determined by use of long-range PCR, as described elsewhere [17, 36]. We also determined whether the GimA-like domain was inserted in the vicinity of the *E. coli* K12 gene *yjiE*, as in archetypal isolate RS218 [31], by PCR amplification of the region between *ibeA* and *yjiE* (2600 bp) with the following primers: *ibeA*.1, 5'-CCG-CCGTTGATGTTATCAAG-3'; and *yjiE*.2, 5'-AACTGGTGAT-CCCGATTTCAG-3'.

We also further characterized a new genomic region defined by 4 different clones obtained by subtractive DNA hybridization between isolate C5 and nonpathogenic isolates (region 4 [50]), designated now GimB in this study (table 1). We first determined the insertion site of this region in isolate C5 by using a PCR-based approach with the following primers: *livJ*.1, 5'-CTTCTGCCAGAGCCATATTG-3'; *TspE4.C4.2*, 5'-AGCTATAGCCGTTTCTACTAAT-3'; and *rpoH*.4, 3'-GACATGACCTTTGACCTGTC-5'. Long-range PCR was used to determine its length and sequence. GimB was screened for in all our isolates by dot blot hybridization, with 4 different subtractive clones, as described elsewhere [50] (table 1). The GimB region was sequenced by the ESGS company (Evry, France). DNA and deduced protein sequences were used to search the DNA and protein databases of the National Center for Biotechnology Information by use of BLAST tools [56]. The sequence of GimB has been submitted to GenBank.

Animal model of meningitis. *E. coli* bacteremia and meningitis were induced by use of representative isolates from the collection. The newborn rat model described by Bortolussi et al. [8] and Kim et al. [10] was adapted, as described elsewhere [35]. Between 10 and 40 animals were infected with each isolate. In brief, pathogen-free Sprague-Dawley rats were obtained from Janvier Laboratories at age 4 days, together with the mothers. At

Table 1. Description of ectochromosomal DNA (ECDNA)-like domains potentially or shown to be involved in the virulence of neonatal *Escherichia coli* meningitis isolates.

ECDNA-like domain	Archetypal strain	Original name of ECDNA (length in kb)	Genes or clones defining the ECDNA-like domains in the present study ^a	Reference
PAI III ₅₃₆ like	UPEC 536	PAI III (~71)	<i>sfa/foc</i> , <i>iroN</i>	[33]
GimA like	MENEC RS218	GimA (20)	<i>ibeA</i> , <i>ptnC</i>	[31]
PAI II _{J96} like	UPEC J96	PAI II (~110)	<i>hlyC</i> , <i>cnf1</i> , <i>hra</i>	[34]
PAI I _{CFT073} like	UPEC CFT073	PAI I (~124)	<i>pap</i> , <i>iucC</i> , <i>hlyC</i>	[38]
HPI like	UPEC 536	PAI IV (38)	<i>irp2</i> , <i>fyuA</i>	[39]
GimB like	MENEC C5	GimB (5.2)	SauE15.L4, SauE15.L9, SauE15.K12, TspE4.C4	This study

NOTE. MENEC, meningitis associated *E. coli*; PAI, pathogenicity island; UPEC, uropathogenic *E. coli*.

^a Clones were obtained by subtractive DNA hybridization in a previous study [50].

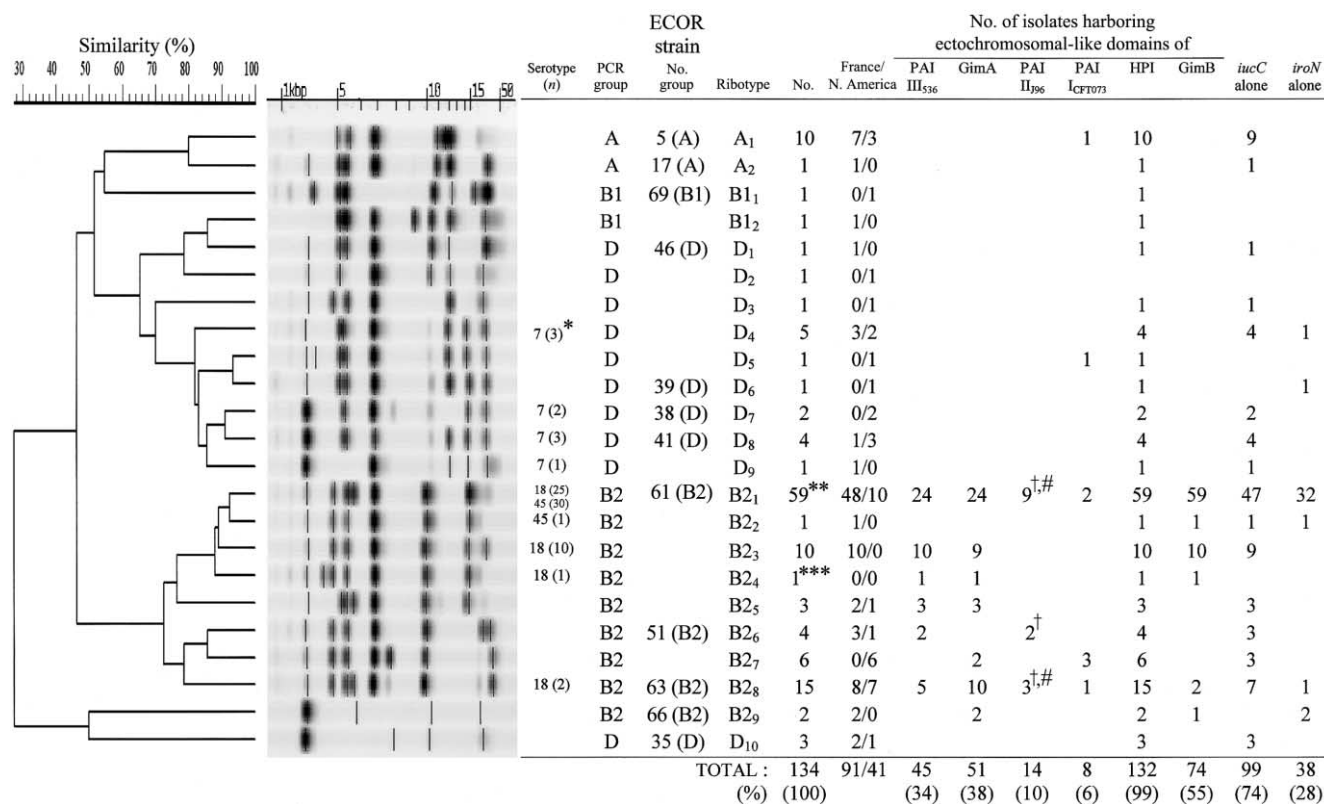


Figure 1. Phylogenetic relationship, ectochromosomal DNA analysis (see table 1 for definitions) and virulence factors distribution among 134 neonatal *Escherichia coli* meningitis isolates. Computerized ribotypes obtained by use of the Riboprinter system were subjected to cluster analysis, and the phylogenetic group (A, B1, B2, and D) was determined by polymerase chain reaction (PCR). Each ribotype was compared to the ribotypes of 72 isolates in the ECOR collection and is designated by its phylogenetic group and a lower-case no. Ribotype prevalences in North America and France also are indicated. *iucC* alone was present but not comprised within a PAI I_{CF073}-like domain, and *iroN* alone was present in a *sfa/fac*-negative isolate. For serotypes, only the distribution and the no. of strains having the serotypes O7:K1; O18:K1, and O45:K1 are shown (*), including archetypal strains C5, RS218 (N. America) and IHE3036 (Finland) (**); PCR *hrra/pheR* fragment size 5.2 kb (†); PCR *hrra/leuX* fragment size 8 kb (‡); and archetypal strain IHE3034 (Finland) (***)

age 5 days, the pups were inoculated intraperitoneally with 200 ± 50 cfu in physiological saline. For each experiment, an inoculum was prepared from the frozen stock of the strain with no more than 1 passage in vitro. Eighteen hours after inoculation, 5 μ L of blood was obtained by tail incision. The animals then were killed, and 5 μ L of CSF was immediately obtained by cisternal puncture. Bacterial counts were determined by culture. The detection limit in blood and CSF was 4×10^2 cfu/mL.

Statistical analysis. Proportions were compared between groups by use of Pearson's χ^2 test or Fisher's exact test, as appropriate. Bacterial counts in the animal model were compared by use of the *t* test. $P < .05$ was considered to denote significant differences. Data are expressed as mean \pm SE.

RESULTS

Phylogenetic analysis and serotypes. To accurately determine the genetic relatedness of the 134 isolates, ribotypes were obtained by use of the automated ribotyping system and were subjected to cluster analysis and comparison to ribotypes of the ECOR

reference strains, in addition to a PCR grouping method. The 134 isolates harbored 23 ribotypes (figure 1), and we observed a perfect identity between automated and manual ribotypes (data not shown). UPGMA cluster analysis revealed that all but 1 of the automated ribotypes linked by a genetic distance of $>65\%$ belonged to the same PCR-based phylogenetic group (figure 1). Moreover, half the ribotypes were identical to the ribotype of 1 of the 72 ECOR reference isolates, corroborating the observed phylogenetic grouping. Each ribotype was thus confidently affiliated to 1 of the major phylogenetic groups and was designated by its group and a lower-case number. Only one ribotype (B1₂), corresponding to a single isolate, could not confidently be affiliated (figure 1). Phylogenetic groups B2, D, A, and B1, respectively accounted for 76%, 15%, 8%, and 1% of the isolates. Four ribotypes (A₁ [$n = 10$], B2₁ [$n = 59$], B2₃ [$n = 10$], and B2₈ [$n = 15$]) accounted for 70% of the isolates, and 11 ribotypes were represented by a single isolate (figure 1). All the ribotypes exhibited by ≥ 3 isolates were found on both continents, except for ribotypes B2₃ ($n = 10$) and B2₇ ($n = 6$), which were restricted to France and North America, respectively. Ribotype di-

versity was higher in North America (15 ribotypes and 41 isolates) than in France (15/ 91). The distribution of phylogenetic groups B2 and D differed significantly between France (81% and 9%, respectively) and North America (61% and 29%, respectively) ($P = .01$ and $P = .002$, respectively), whereas the distribution of phylogenetic groups A and B1 was similar (9% and 1% vs. 7.5% and 2.5%, respectively). Archetypal strains C5, RS218, and IHE3036 belonged to the most frequent ribotype (B_{2,1}), whereas archetypal isolate IHE3034 exhibited the ribotype B_{2,4}, which was represented by this single isolate (figure 1; table 2). The 14.9 kb *Hind*III *rrn*-containing fragment [57] was present in 65% of the 132 isolates and in 73% and 51% of the isolates obtained from France and North America, respectively.

Isolates belonging to the major ribotype (B_{2,1}) were serotyped as were the isolates used in the animal model. Other isolates were screened only for the K1 capsule antigen, the 2 major O antigens encountered worldwide in ECNM isolates (O18 and O7) and O83 (frequent in The Netherlands). Eighty-nine percent of the isolates produced the capsule K1. O18:K1 ($n = 38$) was the most frequent serotype. It was exclusively found in group B2 and mainly ($n = 35$) in the closely related (~90% similarity) ribotypes B_{2,1} and B_{2,3} (figure 1). O7:K1 ($n = 9$) was exclusively found in group D (figure 1). None of the isolate were of the O83:K1 serotype. The serotypes of isolates belonging to the major serotype (B_{2,1}) and the strains used in the animal model are given below.

Characteristics and prevalence of the ECDNA-like domains involved in BBB penetration. Forty-five isolates were found to harbor S-adhesin family genes. Among these 45 isolates, the *sfa/foc* sequence was always physically linked to *iroN* on a frag-

ment ranging in length from 80 kb to 130 kb (figure 2), which suggests the presence of a PAI III₅₃₆-like domain (figure 1). Surprisingly, 3 isolates harbored 2 copies of *sfa/foc*, and, in these 3 isolates, only 1 copy colocalized with the *iro* sequence. Thirty-eight (82%) of the 45 isolates harbored the *sfaS* gene characteristic of S fimbriae (Sfa). The absence of *sfaS* in the remaining 7 isolates (B_{2,1} [$n = 1$], B_{2,6} [$n = 2$], and B_{2,8}, $n = 4$) suggested the presence of another adhesin, such as F1C-fimbriae or S/F1C-related fimbriae. Indeed, using PCR, as described elsewhere [33], we found that 5 of these 7 strains harbored the *focA* gene, specific for F1C-fimbriae (data not shown). Southern hybridization with the *iroN* probe revealed that, among the 45 isolates possessing a PAI III₅₃₆-like domain, 26 isolates harbored an additional copy of *iroN* (figure 2, lane 4). Among the remaining 89 isolates lacking a PAI III₅₃₆-like domain, 38 isolates harbored a copy of *iroN* (figure 1). Hence, 64 (26 + 38) isolates harbored at least 1 copy of *iroN* that was not included in a PAI III₅₃₆-like domain.

All the 51 isolates harboring the *ibeA* gene also harbored *ptnC*, the 2 genes being characteristic of the GimA-like domain (figure 1; table 1). Long-range PCR between *ibeA* and *yjiE* was positive in all 51 isolates, demonstrating that their insertion site was identical to that described in the archetypal isolate RS218.

Genes *hly*, *cnf1*, and *hra*, characteristic of the PAI II₉₆-like domain (table 1), were simultaneously present in 14 isolates and always colocalized on a PFGE fragment varying in length between 210 kb and 700 kb (figure 2). The PAI II₉₆-like domain colocalized with the *pap* sequence in 9 of these 14 isolates. Eight isolates had the *papGIII* allele (like strain J96), and 1 isolate had the *papGII* allele. Thus, *papC* and *papG* were absent from 5 isolates. The insertion site was either *PheR*-tRNA or *LeuX*-tRNA

Table 2. Virulence genotypes defined by different combinations of ectochromosomal DNA (ECDNA) and virulence factors in 54 of 59 isolates harboring ribotype B_{2,1}.

Virulence genotype subgroups	Serotype ^a	Origin	No.	ECDNA-like domains ^b and virulence factors composing the different virulence genotypes						
				PAI III ₅₃₆ like	GimA like	PAI II ₉₆ like	PAI I _{CF1073} like	<i>PapGII</i> alone ^c	<i>iucC</i> alone ^c	<i>iroN</i> alone ^d
I	O45	France	28	–	–	–	–	+	+	+
II	O18	France/N. America	12/1	+	+	–	–	–	+	–
III ^e	O18	N. America	5	+	+	+ ^f	–	–	–	–
IV	O18	France	4	+	+	+ ^g	–	–	+	–
V ^h	O18	Finland/N. America	1/1	+	+	–	–	–	–	–
VI	O1	France	2	–	–	–	+	–	–	+

NOTE. The other 5 of the 59 isolates displayed a unique virulence genotype and were of serotypes O45 ($n = 2$), O1 ($n = 1$), O18 ($n = 1$), and Oauto ($n = 1$). PAI, pathogenicity island.

^a Only O antigens are indicated. All the isolates harbored K1 capsular antigen.

^b See table 1 for definitions.

^c *papG* or *iucC* present but not comprised within a PAI II₉₆- or a PAI I_{CF1073}-like domain.

^d *iroN* present in a *sfa/foc*-negative isolate.

^e This group contained archetypal strains C5 and RS218.

^f PAI II₉₆-like domain inserted in *leuX* tRNA colocalized with the *pap* operon containing the *papGIII* allele.

^g PAI II₉₆-like domain inserted in *PheR* tRNA did not colocalize with the *pap* operon.

^h This group contained archetypal strain IHE3036 (Finland).

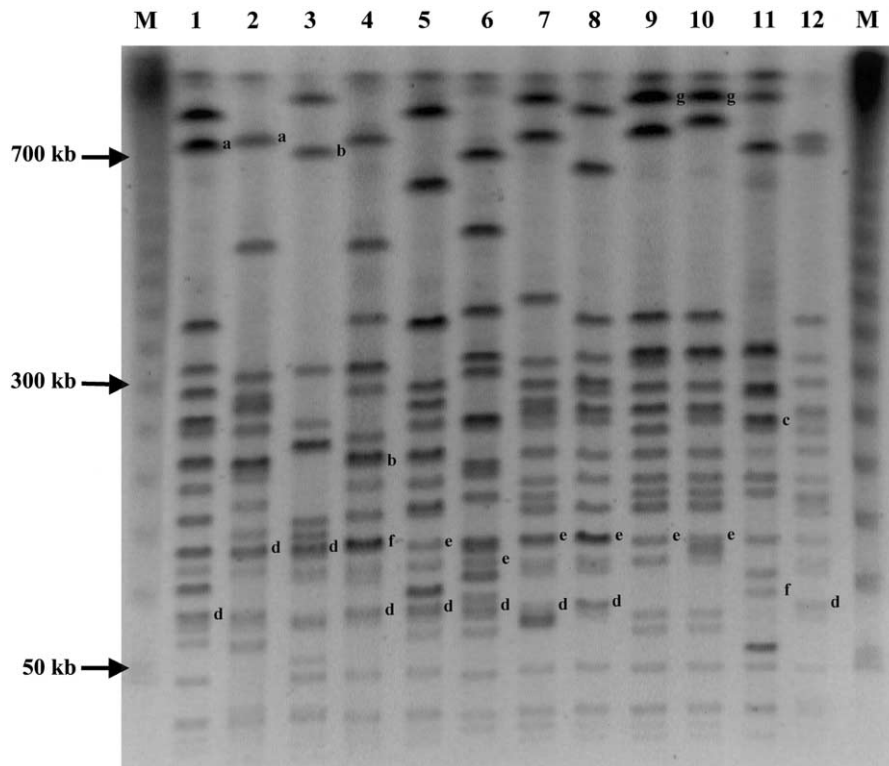


Figure 2. Pulsed-field gel electrophoresis (PFGE) patterns of *NotI*-digested genomic DNA of representative isolates. Localization or colocalization of DNA probes on DNA macrorestriction fragments in Southern hybridization experiments are as follows: A, *papGIII*, *hly*, *cnf1*, and *hra*; B, *hly*, *cnf1*, and *hra*; C, *papGII*, *hly*, and *iucC*; D, *sfa* and *iroN*; E, *iroN* and *iucC*; F, *iroN*; and G, *papGII*. Lane 1, C5 (ribotype B2₁, subgroup III); lane 2, S97 (ribotype B2₃); lane 3, S43 (ribotype B2₂); lane 4, S126 (ribotype B2₁, subgroup IV); lane 5, S44 (ribotype B2₁, subgroup II); lane 6, S94 (ribotype B2₅); lane 7, S3 (ribotype B2₃); lane 8, S46 (ribotype B2₁, subgroup II); lane 9, S88 (ribotype B2₁, subgroup I); lane 10, S95 (ribotype B2₁, subgroup I); lane 11, S34 (ribotype B2₁, subgroup VI); lane 12, S14 (ribotype B2₁, subgroup V); lane M, molecular size marker (50-kb DNA ladder). See figure 1 and table 2 for definitions of ribotypes and subgroups.

in 7 isolates each (figure 1). Interestingly, in the 9 ribotype B2₁ isolates, the insertion site was dependent on the geographical origin; it was *PheR*-tRNA in the 4 French isolates and *LeuX*-tRNA in the 5 North American isolates (see below and table 2).

Thus, PAI III₅₃₆-like, GimA-like, and PAI II₁₉₆-like domains were found in 45 (34%), 51 (38%), and 14 (10%), respectively, of the isolates. These 3 domains were exclusively encountered in phylogenetic group B2, and their distribution did not differ significantly between France and North America.

Characteristics and prevalence of PAI-like domains potentially involved in the bacteremic phase. The distribution of the PAI I_{CFT073}- and HPI-like domains potentially involved in the bacteremic phase of ECNM was different from that of the 3 former ectochromosomal-like domains. PAI I_{CFT073}- and HPI-like domains were encountered in phylogenetic groups A, D, and B2. HPI-like domain was the most frequent ECDNA in our collection (99%). Only 2 isolates, both belonging to phylogenetic group D (ribotypes D₂ and D₄) did not harbor this PAI (figure 1). Whichever the phylogenetic group, the HPI-like domain always was inserted in the vicinity of *asnT*-tRNA. PAI I_{CFT073}, which encodes the siderophore aerobactin, was the least frequent ge-

nomous island-like domain (6%). In contrast, an aerobactin sequence was found outside a PAI I_{CFT073}-like domain in 74% of the isolates (figure 1). Interestingly, when these latter isolates also harbored *iroN* ($n = 67$), the 2 genetic elements always colocalized on a fragment of 120–130 kb in length (figure 2).

Characteristics of a new genomic region. A new genomic region (previously named region 4) [50], defined by 4 different clones (table 1) that were obtained by subtractive DNA hybridization between isolate C5 and nonpathogenic isolates, was further characterized. Multiple amplification with primers homologous to strain K12 genes located in the vicinity of region 4, previously mapped to the chromosome of strain C5 [50], suggested that region 4 was inserted between the *E. coli* K12 genes *livJ* and *rpoH* in isolate C5, because PCR between the 2 genes was negative. Long-range PCR between these 2 genes was positive in strain C5, yielding a fragment of 5.2 kb (data not shown). Sequence analysis of this region 4 gave a G + C content of 39.3% (compared with 50.8% in *E. coli* K12) and identified 6 complete open-reading frames (ORFs). Comparison of the products of these ORFs with database sequences suggested that region 4 contains genes that may be involved in carbohydrate metabolism.

Table 3. Experimental virulence of representative *Escherichia coli* meningitis isolates with the most frequent ribotypes in the different phylogenetic groups.

Isolate	Serotype (ribotype)	Origin	Ecto-chromosomal DNA-like domains ^a and virulence factors							Experimental model, % of rats	
			PAI III ₅₃₆ -like	GimA-like	PAI II ₉₆ -like	HPI-like	GimB-like	<i>iucC</i> alone ^b	<i>iroN</i> alone ^c	Bacteremia, mean log cfu/mL	Meningitis
S82	Ont:K1 ^e (A ₁)	France	–	–	–	+	–	+	–	0	0
S122	O12:K1 (A ₁)	N. America	–	–	–	+	–	+	–	0	0
S16	O7:K1 (D ₄)	N. America	–	–	–	+	–	+	–	50 (3.7) ^d	8 ^d
S18	O7:K1 (D ₈)	N. America	–	–	–	+	–	+	–	80 (4.7) ^d	50
C5	O18:K1 (B2 ₁)	N. America	+	+	+	+	+	–	–	100 (5.7)	52
S88	O45:K1 (B2 ₁)	France	–	–	–	+	+	+	+	100 (6.4) ^d	69
S95	O45:K1 (B2 ₁)	France	–	–	–	+	+	+	+	100 (7.3) ^d	93 ^d

^a See table 1 for definitions.

^b *iucC* present but not comprised within a PAI I_{CFT073}-like domain.

^c *iroN* present in a *sfa/foc*-negative isolate.

^d $P < .05$, vs. strain C5 (t test for mean; χ^2 test for percentage).

^e Nontypeable.

The ORF-1 to ORF-4 products showed homologies with phosphotransferase system proteins (*Salmonella typhi*; accession nos. NP 458163 to NP 458165; 60%–66% aa similarity). ORF 5 and ORF 6 showed homologies with proteins with phosphoglycerate dehydrogenase (*Methanocaldococcus jannaschii*; accession no. NP 248012.1; 55% aa similarity) and dihydrodipicolinate synthase activities (*Bacillus halodurans*; accession no. NP 242608; 55% aa similarity), respectively. No mobility loci (e.g., IS and integrase) and no repeat structures similar to those characteristics of PAI were found. Finally, no tRNA genes were found in the flanking regions. This region then was named GimB (genetic island of meningitic *E. coli*) in keeping with the nomenclature of Huang et al. [31]. GimB was screened for by dot blot hybridization, with 4 different subtractive clones (table 1) and was found in 74 (55%) of our isolates (exclusively in group B2). PCR of the junction region, between *livJ* and TspE4.C4 was positive in all 74 isolates, indicating an identical insertion site. The prevalence of GimB in group B2 (74%) was significantly higher than that of the PAI III₅₃₆-like domain (45%) and the GimA-like domain (51%) ($P < .001$).

Nucleotide sequence accession number. We deposited the complete GimB nucleotide sequence in the GenBank nucleotide sequence data library under accession number AY170898.

Characteristics of the major ribotype. Fifty-nine isolates belonged to ribotype B2₁ (48 from all the regions of France, 10 from North America, and the archetypal strain IHE3036 from Finland) and represented 44% of our isolate collection. This group of isolates was subdivided on the basis of the distribution of ECDNA-like domains and virulence factors defining the virulence genotypes (table 2). The serotype of each isolate also was determined. Six subgroups (I–VI), each containing at least 2 isolates, are described in table 2. The characteristics of the different subgroups were as follows. Subgroup I ($n = 28$) was en-

countered exclusively in different parts of France and alone represented almost one-third of french isolates. These isolates harbored the genes *iucC*, *iroN*, and *papGII*, and none harbored an ECDNA-like domain involved in BBB penetration (table 2). Interestingly, all these isolates differed by only 2–5 bands on PFGE (data not shown) and belong to the rare serotype O45:K1, whereas the isolates belonging to the other subgroups were serotype O18:K1 or O1:K1 (table 2). The 13 subgroup II isolates (O18:K1) harbored a PAI III₅₃₆-like domain, a GimA-like domain, and the aerobactin sequence. This was the only subgroup to comprise isolates from both North America and France. Subgroup III (O18:K1) contained 5 isolates (including the archetypal isolates C5 and RS218) and was found only in North America. This subgroup harbored a PAI II₉₆-like domain that colocalized with the *pap* operon (containing the *papGIII* allele and inserted in the *leuX* tRNA gene). In contrast, subgroup IV, found exclusively in France, resembled subgroup III, except that it harbored *iucC* and a PAI II₉₆-like domain (without the *pap* operon) inserted in the *pheR*-tRNA gene (table 2). Subgroup V resembled also to subgroup III but lacked the PAI II₉₆-like domain. It contained only 2 isolates (O18:K1), one of which was the archetypal isolate IHE3036. Subgroup VI was the only one to contain isolates of serotype O1:K1 and to harbor PAI I_{CFT073}-like domains.

Experimental virulence. To identify a possible correlation between the isolates' genetic background and virulence genotype on one hand and their capacity to induce bacteremia and meningitis on the other hand, we tested representative isolates in a rat model of neonatal meningitis (table 3). Two representative isolates were selected from each phylogenetic group A, D, and B2, and were compared with reference strain C5 (table 3). The panel isolates were chosen because they belonged to the 1 or 2 of the most common ribotypes in each phylogenetic

group and harbored the most frequent virulence gene pattern in the relevant ribotype.

With the archetypal strain C5 (ribotype B2₁; virulence genotype subgroup III), all the rats were bacteremic 18 h after challenge; the level of bacteremia was 5.7 ± 0.25 log cfu/mL, and 52% of the animals had meningitis. Isolates S88 and S95 (both O45:K1), belonging to the same ribotype (B2₁) and displaying the virulence genotype of subgroup I, yielded significantly higher bacteremia (6.4 ± 0.37 and 7.3 ± 0.6 log cfu/mL, respectively; $P < .05$ for both), and isolates S95 gave a significantly higher rate of meningitis (93%; $P < .05$ vs. isolate C5; table 3). With isolates S16 and S18, both belonging to phylogenetic group D and serotype O7:K1, bacteremia was less frequent than with isolate C5 (50% and 80%, respectively) and also significantly less severe (3.7 ± 0.3 and 4.7 ± 1.1 log cfu/mL; $P < .05$; table 3). Probably as a consequence of the lower level of bacteremia, meningitis was less frequently observed with S16 than with C5 (table 3). Finally, isolates S82 and S122, belonging to phylogenetic group A, failed to induce bacteremia (table 3). With these latter isolates, bacteremia was only obtained when the inoculum was increased 1000-fold (data not shown).

DISCUSSION

Over the past few years, major progress has been made in the understanding of the pathophysiology of ECNM. In particular, specific virulence factors have been identified and are now known to be carried on ECDNA in most cases. However, most relevant studies have been performed on a limited number of strains, most of which belonged to the so-called archetypal group O18:K1, the main serotype encountered in this disease [41, 47–49]. Little is known of the molecular pathophysiology of isolates belonging to other important serotypes, such as O7:K1 (encountered in Europe and North American) and O83:K1 (mainly described in The Netherlands) [47–49]. Such investigations require representative virulent isolates among the different clusteral or clonal groups. Indeed, one-third of cases of ECNM occur in premature neonates [49], who are immunologically immature [58] and thus may be infected by less virulent strains [40, 59]. Unfortunately, such clinical data are generally unavailable in ECNM isolate collections. One way to clarify this issue is to use a reproducible experimental model to evaluate the intrinsic virulence of bacterial isolates. Here, we report for the largest intercontinental collection of ECNM isolates to date the results of (1) phylogenetic analysis, (2) distribution of virulence factor genes and ECDNA-like domains, and (3) experimental virulence.

To optimize the phylogenetic analysis, we used both automated ribotyping and a PCR-based grouping method. The use of standardized Riboprinter methodology permitted rigorous comparison of all the patterns obtained, as well as a comparison with those of isolates belonging to the ECOR reference collec-

tion that we have described elsewhere [53]. Few previous studies have focused on the distribution of the 4 phylogenetic groups of extraintestinal pathogenic *E. coli* [36, 40, 41, 44]. Our results confirm the predominance of groups B2 and D and the minor contribution of groups B1/A. The proportion of B2/D isolates was similar in France (90%) and North America (90%), but a higher proportion of group B2 isolates were observed in France (81%) than in North America (61%). A similar high proportion of group B2 isolates (81%) was found by Johnson et al. [41] among 70 ECNM isolates from the Netherlands. This marked predominance of group B2 isolates in France and in The Netherlands could be due to clonal expansion of a group of serotype O45:K1 and O83:K1 isolates, respectively [41, 49]. In the study by Johnson et al. [41], the prevalence of phylogenetic groups A and B1 differed from that found in our study in France (A, 1% vs. 9% [$P = .07$]; B1, 10% vs. 1%, [$P = .02$]). Johnson et al. [41] found that group B1 was the second largest group after group B2, whereas group B1 was the smallest group in our ECNM collection in both France and North America. This difference may be explained by the different geographic source or by differences in host status between the 2 studies. However, our results strongly suggest that B1 is the phylogenetic group with the lowest extraintestinal virulence. This is in agreement with the rarity of extraintestinal virulence genes found in group B1 isolates of the ECOR reference collection [40, 46, 60] and from fecal microflora [61]. The rarity of group B1 ECNM isolates is also in accordance with the very low frequency of group B1 uropathogenic *E. coli* isolates that we have previously observed, as described elsewhere [36].

The discovery of ECDNA involved in pathogenicity is changing the epidemiological approach to virulence factors in pathogenic strain collections. Most of these structures are composed of several virulence factors [30], which is unlikely to be a chance occurrence. On the contrary, some virulence factors may be juxtaposed on the bacterial chromosome, because they may act synergistically at a particular pathophysiological step. Thus, although PAIs may show variability due to deletion or insertion of virulence factor genes, some of the genes may be interdependent and thus constitute a “signature” or “backbone” of a given ECDNA. For example, after studying the characteristic virulence factor genes comprising PAI II₉₆ in *E. coli* urosepsis isolates, we recently found that *hly*, *cnf1*, and *hra* were consistently physically linked, which suggests that they may form the backbone of the PAI and, possibly, a virulence entity [36]. In the present study, we again found that *hly*, *cnf1*, and *hra* always colocalized in the 14 isolates that harbored these 3 genes. This was not due to a clonal distribution of this PAI-like domain, because the 14 isolates belonged to 3 different ribotypes and because the PAI-like domain was inserted at 2 different sites. Of interest, 5 of the 14 isolates did not harbor the *pap* operon described in the archetypal PAI II₉₆. This feature, also observed

in some urosepsis isolates [36] and probably in adult bacteremia strains [62], illustrates PAI variability (probably due in this case to deletion or insertion of the *pap* operon between the *cnf1* and *hra* genes) that was suggested by analyzing the co-occurrence of these genes in extraintestinal *E. coli* strains [43, 63].

The PAI III₅₃₆-like domain, which we defined by *sfa/foc* and *iroN* colocalization, was found in 34% of our isolates and is another example of a putative PAI backbone. Dobrindt et al. [33], using a PCR-based approach, found that isolates harboring the genetic determinants coding for different members of the S-adhesin family always harbored the *iro* locus. We confirmed this finding and also demonstrated that *sfa/foc* and *iro* sequences are physically linked in isolates harboring both genes. In contrast, 38 (28%) isolates harbored *iro* but not *sfa/foc* sequences, similarly to urosepsis isolates [12]. Our results thus reconcile the apparently conflicting findings of Dobrindt et al. [33] and Johnson et al. [12]. The consistent cotransfer of these both genes when *sfa* is present in isolates harboring 6 different ribotypes may indicate an “*iroN* dependency” of the *sfa* operon for virulence expression. On the other hand, the presence of *iroN* without *sfa/foc* suggests that the former gene may play a role in virulence independently of *sfa/foc*. Likewise, the consistent colocalization of *iroN* and *iucC* in isolates harboring both genes, as well as their position on a fragment of <130 kb, suggests that the *iro* locus is borne on a plasmid. This supports work from Johnson et al. [12], who found a statistical association between *iro* and *traT*, a plasmid-borne gene. This putative location of *iroN* on a plasmid would explain why this gene (not linked to *sfa/foc*) is present in phylogenetic groups D and B2, whereas *iroN* sequences included in PAI III₅₃₆ are found only in group B2 (figure 1). Finally, we also found, for the first time, that 2 copies of *iroN* could be simultaneously present (26 of the 83 *iroN*-positive isolates). It is likely that this duplication concerns the entire locus *iro* and not only the *iroN* gene, because hybridization of PFGE Southern with a probe homologous to the *iroC* gene gave identical results (data not shown). To our knowledge, no other iron uptake system has been previously found with such a rate of duplication. Although specific studies are required, this last finding argues in favor of a key role of *iroN* in iron acquisition and, thus, in the virulence of ECNM isolates.

Our extensive analysis of virulence factors, both singly and in specific combinations in the O18:K1 strain group revealed that, although certain virulence determinants were variably present (PAI II₁₉₆ [24%] and *iucC* [76%]), some others, such as PAI III₅₃₆ and GimA, had a very high prevalence (92% each). Johnson et al. [64], studying O18:K1 cystitis isolates belonging to the subclone OMP6, found the prevalence rates of *ibeA* (comprised in GimA) and *papGIII* (probably comprised in PAI II₁₉₆) to be 40% and 100%, respectively ($P < .001$ for both). It may be hypothesized that the genetic background of bacteria

of clonal group O18:K1 may be favorable for the development of extraintestinal virulence specialization, uropathogenicity being conferred in part by acquisition of *papGIII* via PAI II₁₉₆ and meningitis by the acquisition notably of GimA. Moreover, it might be possible for some strains to acquire both specialization sequentially, and we believe that C5 and RS218 strains are representative of these. It should be noted that this hypothesis of double valence is of clinical relevance since it is known that 20% of cases of neonatal meningitis are a complication of urinary tract infection [65, 66].

One of the major findings in this study was the discovery of a highly virulent clonal group (ribotype B2₁, subgroup I) of French isolates harboring the same virulence determinants and representing almost one-third of French isolates in our collection. Surprisingly, this clone was serotype O45:K1, which, to our knowledge, has not been described previously in ECNM isolates, except in Hungary [67] and during 2 outbreaks in Germany [68]. It has been reported only rarely in the fecal microflora of infants and adults [51, 69] and as an avian pathogen [51, 68]. Of interest, strains of human origin described by Wullenweber et al. [69] and Ott et al. [51] were similar to our isolates, P-fimbriae and aerobactin positive, and S fimbriae and hemolysin negative, which suggests the presence of the same clone throughout Europe. We found that 2 isolates (S88 and S95) representative of this clone and with different pulsed types (figure 2) had at least the same capacity as strain C5 to induce bacteremia and meningitis in our experimental model, although they did not harbor any of the ECDNA-like domains implicated in BBB penetration. This is of major concern, because these results suggest that BBB-penetration mechanisms other than *sfaS*-mediated adhesion and *cnf1*- and *ibeA*-mediated endothelial cell invasion have developed in this clonal group of strains, phylogenetically related to archetypal strains (ribotype B2₁). It is possible that the significantly higher level of bacteremia induced by S88 and S95 relative to C5 facilitates their BBB passage. To explain this high level of bacteremia, we first examined the resistance of these strains to serum bactericidal activity. Preliminary results suggest that strain C5 and the O45:K1 isolates do not significantly differ in this respect and thus, that other mechanisms account for the high level of bacteremia in the O45:K1 strains (data not shown).

Also of particular interest was the marked difference in the capacity of isolates S88 and S95 and the O7:K1 isolates S16 and S18 (phylogenetic group D) to induce bacteremia. Except for the genetic island GimB and the *iroN* gene, which were only present in isolates S88 and S95, all 4 isolates harbored the same virulence genes known or potentially involved in the bacteremic phase, such as polysaccharide K1, HPI, and aerobactin (table 3). The lesser pathogenicity of the O7:K1 isolates is in agreement with data from Pluschke et al. [70], who showed in an animal model that O7:K1 isolates from diverse sources were

less virulent than O18:K1 strains in regards to mortality. Although our results may be explained by differences in the lipopolysaccharides expressed by these isolates (O45 vs. O7), they also suggest that GimB or the iron uptake system encoded by *iroN* may be involved in the sustained high level of bacteremia that characterizes ECNM.

The experimental virulence of isolates belonging to group A also was noteworthy. The 11 group A isolates, found on both continents, had similar virulence genotypes, most expressing polysaccharide K1 (73%), HPI (100%), and aerobactin (100%). The prevalence of this virulence genotype was higher than among group A isolates of the ECOR collection (4%, 32%, and 24%, respectively) [17, 60]. These 11 isolates may thus constitute an atypical virulence group among group A isolates, which are generally defined as commensals. The 2 isolates representative of group A, S122 from North America and S82 from France, were avirulent in our animal model, which suggests that, although capsular K1, HPI, and aerobactin may be a prerequisite for extraintestinal virulence, they are not sufficient to transform a commensal into a meningitis-causing strain. Thus, group A isolates harboring these virulence factors would probably only cause meningitis in vulnerable neonates. In our opinion, phylogenetic grouping of ECNM isolates, which is now relatively easy [52], should be done routinely. Detection of a group A isolate causing infection in a normal-risk neonate may point to a immune deficiency. This may also apply to the extremely rare group B1 isolates.

In conclusion, our results demonstrate that the known ECDNA elements discovered in archetypal ECNM strains do not fully explain the pathophysiology of bacteremia and the traversal of the BBB during *E. coli* meningitis. Current archetypal meningitis strains appear to be only partially representative of the pathogenic mechanisms harbored by *E. coli* meningitis isolates. The highly virulent O45:K1 clonal group of ECNM isolates found in our study may serve to identify new virulence factors and other genetic determinants that contribute to in vivo fitness, by enhancing bacterial survival and transmissibility. It also may serve to find common pathogenic mechanisms among different ECNM clonal groups that may be used as potential target for a worldwide efficacious prevention strategy.

Acknowledgments

We thank L. Beutin (Division of Emerging Bacterial Pathogens, Robert Koch-Institut, Berlin, Germany), who kindly detected the serotype of the new O45:K1 clone on a set of 4 isolates; H. Dabernat, M. Thibaut, H. Chardon, J. C. Philippe, J. Freney, T. Lambert, J. Raymond, M. Weber, H. Vu Thien, K. Kim, J. Badger, J. Hacker, R. Bortolussi, D. Goldmann, and R. Selander, for providing some of the isolates used in this study; Maryse De-Ré (Institut Pasteur de Lille), for her valuable tech-

nical assistance; Qualicon Europe, for providing the Riboprinter reagents used in this work; and Y. Aujard, for enlightening nightly discussion on *Escherichia coli* neonatal infections.

References

1. Stoll BJ. The global impact of neonatal infection. *Clin Perinatol* **1997**; 24:1–21.
2. Schrag SJ, Zywicki S, Farley MM, et al. Group B streptococcal disease in the era of intrapartum antibiotic prophylaxis. *N Engl J Med* **2000**; 342:15–20.
3. Joseph TA, Pyati SP, Jacobs N. Neonatal early-onset *Escherichia coli* disease: the effect of intrapartum ampicillin. *Arch Pediatr Adolesc Med* **1998**; 152:35–40.
4. Stoll BJ, Hansen N, Fanaroff AA, et al. Changes in pathogens causing early-onset sepsis in very-low-birth-weight infants. *N Engl J Med* **2002**; 347:240–7.
5. Towers CV, Carr MH, Padilla G, Asrat T. Potential consequences of widespread antepartal use of ampicillin. *Am J Obstet Gynecol* **1998**; 179: 879–83.
6. Dietzman DE, Fischer GW, Schoenknecht FD. Neonatal *Escherichia coli* septicemia: bacterial counts in blood. *J Pediatr* **1974**; 85:128–30.
7. Glode MP, Sutton A, Moxon ER, Robbins JB. Pathogenesis of neonatal *Escherichia coli* meningitis: induction of bacteremia and meningitis in infant rats fed *Escherichia coli* K1. *Infect Immun* **1977**; 16:75–80.
8. Bortolussi R, Ferrieri P, Wannamaker LW. Dynamics of *Escherichia coli* infection and meningitis in infant rats. *Infect Immun* **1978**; 22:480–5.
9. Kim KS. *Escherichia coli* translocation at the blood-brain barrier. *Infect Immun* **2001**; 69:5217–22.
10. Kim KS, Itabashi H, Gemski P, Sadoff J, Warren RL, Cross AS. The K1 capsule is the critical determinant in the development of *Escherichia coli* meningitis in the rat. *J Clin Invest* **1992**; 90:897–905.
11. Pluschke G, Mayden J, Achtman M, Levine RP. Role of the capsule and the O antigen in resistance of O18:K1 *Escherichia coli* to complement-mediated killing. *Infect Immun* **1983**; 42:907–13.
12. Johnson JR, Russo TA, Tarr PI, et al. Molecular epidemiological and phylogenetic associations of two novel putative virulence genes, *iha* and *iroN_{E. coli}*, among *Escherichia coli* isolates from patients with urosepsis. *Infect Immun* **2000**; 68:3040–7.
13. Russo TA, Carlino UB, Mong A, Jodush ST. Identification of genes in an extraintestinal isolate of *Escherichia coli* with increased expression after exposure to human urine. *Infect Immun* **1999**; 67:5306–14.
14. Torres AG, Payne SM. Haem iron-transport system in enterohaemorrhagic *Escherichia coli* O157:H7. *Mol Microbiol* **1997**; 23:825–33.
15. Johnson JR. Virulence factors in *Escherichia coli* urinary tract infection. *Clin Microbiol Rev* **1991**; 4:80–128.
16. Carniel E. The *Yersinia* high-pathogenicity island: an iron-uptake island. *Microbes Infect* **2001**; 3:561–9.
17. Clermont O, Bonacorsi S, Bingen E. The *Yersinia* high-pathogenicity island is highly predominant in virulence-associated phylogenetic groups of *Escherichia coli*. *FEMS Microbiol Lett* **2001**; 196:153–7.
18. Schubert S, Rakin A, Karch H, Carniel E, Heesemann J. Prevalence of the “high-pathogenicity island” of *Yersinia* species among *Escherichia coli* strains that are pathogenic to humans. *Infect Immun* **1998**; 66:480–5.
19. Bhakdi S, Muhly M, Korom S, Schmidt G. Effects of *Escherichia coli* hemolysin on human monocytes: cytotoxic action and stimulation of interleukin 1 release. *J Clin Invest* **1990**; 85:1746–53.
20. May AK, Gleason TG, Sawyer RG, Pruett TL. Contribution of *Escherichia coli* α -hemolysin to bacterial virulence and to intraperitoneal alterations in peritonitis. *Infect Immun* **2000**; 68:176–83.
21. Welch RA, Dellinger EP, Minshew B, Falkow S. Hemolysin contributes to virulence of extra-intestinal *Escherichia coli* infections. *Nature* **1981**; 294:665–7.
22. Hoffman JA, Wass C, Stins MF, Kim KS. The capsule supports survival

- but not traversal of *Escherichia coli* K1 across the blood-brain barrier. *Infect Immun* **1999**;67:3566–70.
23. Parkkinen J, Korhonen TK, Pere A, Hacker J, Soinila S. Binding sites in the rat brain for *Escherichia coli* S fimbriae associated with neonatal meningitis. *J Clin Invest* **1988**;81:860–5.
 24. Stins MF, Prasadarao NV, Ibric L, Wass CA, Luckett P, Kim KS. Binding characteristics of S fimbriated *Escherichia coli* to isolated brain microvascular endothelial cells. *Am J Pathol* **1994**;145:1228–36.
 25. Korhonen TK, Valtonen MV, Parkkinen J, et al. Serotypes, hemolysin production, and receptor recognition of *Escherichia coli* strains associated with neonatal sepsis and meningitis. *Infect Immun* **1985**;48:486–91.
 26. Huang SH, Wan ZS, Chen YH, Jong AY, Kim KS. Further characterization of *Escherichia coli* brain microvascular endothelial cell invasion gene *ibeA* by deletion, complementation, and protein expression. *J Infect Dis* **2001**;183:1071–8.
 27. Huang SH, Wass C, Fu Q, Prasadarao NV, Stins M, Kim KS. *Escherichia coli* invasion of brain microvascular endothelial cells in vitro and in vivo: molecular cloning and characterization of invasion gene *ibe10*. *Infect Immun* **1995**;63:4470–5.
 28. Khan NA, Wang Y, Kim KJ, Chung JW, Wass CA, Kim KS. Cytotoxic necrotizing factor–1 contributes to *Escherichia coli* K1 invasion of the central nervous system. *J Biol Chem* **2002**;277:15607–12.
 29. Badger JL, Wass CA, Weissman SJ, Kim KS. Application of signature-tagged mutagenesis for identification of *Escherichia coli* K1 genes that contribute to invasion of human brain microvascular endothelial cells. *Infect Immun* **2000**;68:5056–61.
 30. Hacker J, Blum-oebler J, Janke B, Nagy G, Hoebel W. Pathogenicity islands of extraintestinal *Escherichia coli*. In: Kaper JB, Hacker J, eds. Pathogenicity islands and other mobile virulence elements. Washington, DC: American Society for Microbiology Press, **1999**:59–76.
 31. Huang SH, Chen YH, Kong G, et al. A novel genetic island of meningitic *Escherichia coli* K1 containing the *ibeA* invasion gene (GimA): functional annotation and carbon-source–regulated invasion of human brain microvascular endothelial cells. *Funct Integr Genomics* **2001**;1:312–22.
 32. Welch RA, Redford P. Extraintestinal *Escherichia coli* as a model system for the study of pathogenicity islands. In: Hacker J, Kaper JB, eds. Pathogenicity islands and the evolution of pathogenic microbes. Vol. 1. Berlin: Springer, **2002**:15–30.
 33. Dobrindt U, Blum-Oehler G, Hartsch T, et al. S-Fimbria–encoding determinant *sfa(I)* is located on pathogenicity island III₅₃₆ of uropathogenic *Escherichia coli* strain 536. *Infect Immun* **2001**;69:4248–56.
 34. Swenson DL, Bukanov NO, Berg DE, Welch RA. Two pathogenicity islands in uropathogenic *Escherichia coli* J96: cosmid cloning and sample sequencing. *Infect Immun* **1996**;64:3736–43.
 35. Houdouin V, Bonacorsi S, Brahim N, Clermont O, Nassif X, Bingen E. A uropathogenicity island contributes to the pathogenicity of *Escherichia coli* strains that cause neonatal meningitis. *Infect Immun* **2002**;70:5865–9.
 36. Bingen-Bidois M, Clermont O, Bonacorsi S, et al. Phylogenetic analysis and prevalence of urosepsis strains of *Escherichia coli* bearing pathogenicity island-like domains. *Infect Immun* **2002**;70:3216–26.
 37. Carniel E, Guilyoule A, Guilvout I, Mercereau-Puijalon O. Molecular cloning, iron-regulation and mutagenesis of the *irp2* gene encoding HMWP2, a protein specific for the highly pathogenic *Yersinia*. *Mol Microbiol* **1992**;6:379–88.
 38. Guyer DM, Kao JS, Mobley HL. Genomic analysis of a pathogenicity island in uropathogenic *Escherichia coli* CFT073: distribution of homologous sequences among isolates from patients with pyelonephritis, cystitis, and catheter-associated bacteriuria and from fecal samples. *Infect Immun* **1998**;66:4411–7.
 39. Schubert S, Rakin A, Fischer D, Sorsa J, Heesemann J. Characterization of the integration site of *Yersinia* high-pathogenicity island in *Escherichia coli*. *FEMS Microbiol Lett* **1999**;179:409–14.
 40. Bingen E, Picard B, Brahim N, et al. Phylogenetic analysis of *Escherichia coli* strains causing neonatal meningitis suggests horizontal gene transfer from a predominant pool of highly virulent B2 group strains. *J Infect Dis* **1998**;177:642–50.
 41. Johnson JR, Oswald E, O'Bryan TT, Kuskowski MA, Spanjaard L. Phylogenetic distribution of virulence-associated genes among *Escherichia coli* isolates associated with neonatal bacterial meningitis in The Netherlands. *J Infect Dis* **2002**;185:774–84.
 42. Johnson JR, Goulet P, Picard B, Moseley SL, Roberts PL, Stamm WE. Association of carboxylesterase B electrophoretic pattern with presence and expression of urovirulence factor determinants and antimicrobial resistance among strains of *Escherichia coli* that cause urosepsis. *Infect Immun* **1991**;59:2311–5.
 43. Johnson JR, Stell AL. Extended virulence genotypes of *Escherichia coli* strains from patients with urosepsis in relation to phylogeny and host compromise. *J Infect Dis* **2000**;181:261–72.
 44. Johnson JR, Kuskowski MA, O'Bryan TT, Maslow JN. Epidemiological correlates of virulence genotype and phylogenetic background among *Escherichia coli* blood isolates from adults with diverse-source bacteraemia. *J Infect Dis* **2002**;185:1439–47.
 45. Picard B, Garcia JS, Gouriou S, et al. The link between phylogeny and virulence in *Escherichia coli* extraintestinal infection. *Infect Immun* **1999**;67:546–53.
 46. Boyd EF, Hartl DL. Chromosomal regions specific to pathogenic isolates of *Escherichia coli* have a phylogenetically clustered distribution. *J Bacteriol* **1998**;180:1159–65.
 47. Achtman M, Mercer A, Kusecek B, et al. Six widespread bacterial clones among *Escherichia coli* K1 isolates. *Infect Immun* **1983**;39:315–35.
 48. Sarff LD, McCracken GH, Schiffer MS, et al. Epidemiology of *Escherichia coli* K1 in healthy and diseased newborns. *Lancet* **1975**;1:1099–104.
 49. Mulder CJ, van Alphen L, Zanen HC. Neonatal meningitis caused by *Escherichia coli* in The Netherlands. *J Infect Dis* **1984**;150:935–40.
 50. Bonacorsi S, Clermont O, Tinsley C, et al. Identification of regions of the *Escherichia coli* chromosome specific for neonatal meningitis-associated strains. *Infect Immun* **2000**;68:2096–101.
 51. Ott M, Bender L, Blum G, et al. Virulence patterns and long-range genetic mapping of extraintestinal *Escherichia coli* K1, K5, and K100 isolates: use of pulsed-field gel electrophoresis. *Infect Immun* **1991**;59:2664–72.
 52. Clermont O, Bonacorsi S, Bingen E. Rapid and simple determination of the *Escherichia coli* phylogenetic group. *Appl Environ Microbiol* **2000**;66:4555–8.
 53. Clermont O, Cordevant C, Bonacorsi S, Marecat A, Lange M, Bingen E. Automated ribotyping provides rapid phylogenetic subgroup affiliation of clinical extraintestinal pathogenic *Escherichia coli* strains. *J Clin Microbiol* **2001**;39:4549–53.
 54. Dice LR. Measures of the amount of ecological associations between species. *J Ecology* **1945**;26:297–302.
 55. Ochman H, Selander RK. Standard reference strains of *Escherichia coli* from natural populations. *J Bacteriol* **1984**;157:690–3.
 56. Altschul SF, Madden TL, Schaffer AA, et al. Gapped BLAST and PSI-BLAST: a new generation of protein database search programs. *Nucleic Acids Res* **1997**;25:3389–402.
 57. Bingen E, Denamur E, Brahim N, Elion J. Genotyping may provide rapid identification of *Escherichia coli* K1 organisms that cause neonatal meningitis. *Clin Infect Dis* **1996**;22:152–6.
 58. Wilson CB. Immunologic basis for increased susceptibility of the neonate to infection. *J Pediatr* **1986**;108:1–12.
 59. Tullus K, Brauner A, Fryklund B, et al. Host factors versus virulence-associated bacterial characteristics in neonatal and infantile bacteraemia and meningitis caused by *Escherichia coli*. *J Med Microbiol* **1992**;36:203–8.
 60. Johnson JR, Delavari P, Kuskowski M, Stell AL. Phylogenetic distribution of extraintestinal virulence-associated traits in *Escherichia coli*. *J Infect Dis* **2001**;183:78–88.
 61. Duriez P, Clermont O, Bonacorsi S, et al. Commensal *Escherichia coli* isolates are phylogenetically distributed among geographically distinct human populations. *Microbiology* **2001**;147:1671–6.

62. Hilali F, Ruimy R, Saulnier P, et al. Prevalence of virulence genes and clonality in *Escherichia coli* strains that cause bacteremia in cancer patients. *Infect Immun* **2000**; 68:3983–9.
63. Johnson JR, O'Bryan TT, Kuskowski M, Maslow JN. Ongoing horizontal and vertical transmission of virulence genes and papA alleles among *Escherichia coli* blood isolates from patients with diverse-source bacteremia. *Infect Immun* **2001**; 69:5363–74.
64. Johnson JR, Delavari P, O'Bryan TT. *Escherichia coli* O18:K1:H7 isolates from patients with acute cystitis and neonatal meningitis exhibit common phylogenetic origins and virulence factor profiles. *J Infect Dis* **2001**; 183: 425–34.
65. Unhanand M, Mustafa MM, McCracken GH, Jr., Nelson JD. Gram-negative enteric bacillary meningitis: a twenty-one-year experience. *J Pediatr* **1993**; 122:15–21.
66. Bachur R, Caputo GL. Bacteremia and meningitis among infants with urinary tract infections. *Pediatr Emerg Care* **1995**; 11:280–4.
67. Czirik E, Herpay M, Milch H. Computerized complex typing of *Escherichia coli* strains from different clinical materials. *Acta Microbiol Hung* **1993**; 40:217–37.
68. Tschäpe H, Steinrück H, Buchholz P, et al. Molecular analysis of *Escherichia coli* from neonatal infections and its epidemiological implication. In: Gravel E, Stern L, Syllim-Rapoport I, Waver R, eds. *Research in perinatal medicine II*. Berlin: Verlag Gesundheit, **1990**:224–34.
69. Wullenweber M, Beutin L, Zimmermann S, Jonas C. Influence of some bacterial and host factors on colonization and invasiveness of *Escherichia coli* K1 in neonatal rats. *Infect Immun* **1993**; 61:2138–44.
70. Pluschke G, Mercer A, Kusecek B, Pohl A, Achtman M. Induction of bacteremia in newborn rats by *Escherichia coli* K1 is correlated with only certain O lipopolysaccharide antigen types. *Infect Immun* **1983**; 39: 599–608.

In an article in the 1 September 2003 issue of the *Journal* (Fischl MA, Ribaud HJ, Collier AC, et al. A Randomized Trial of 2 Different 4-Drug Antiretroviral Regimens versus 3-Drug Regimen, in *Advanced Human Immunodeficiency Virus Disease* (J Infect Dis 2003;188:625–34), the list of authors should have included the following 2 individuals: Lisa M. Demeter and Susan H. Eshleman. Dr. Demeter's affiliation is Division of Infectious

In an article in the 15 June 2003 issue of the *Journal* (Bonacorsi S, Clermont O, Houdouin V, et al. Molecular Analysis and Experimental Virulence of French and North American *Escherichia coli* Neonatal Meningitis Isolates: Identification of a New Virulent Clone. J Infect Dis 2003;187:1895–1906), there is an error in line

Diseases, University of Rochester, Rochester, New York; Dr. Eshleman's affiliation is Department of Pathology, Johns Hopkins Medical Institutions, Baltimore, Maryland. The authors regret this error.

12 of the right-hand column on page 1896; the numeral should be 6 (rather than 9), so that the "which" clause beginning on line 11 reads as "which belong to the outer membrane protein pattern (OMP) 6 subclone." The authors regret this error.